PCCP

Cite this: *Phys. Chem. Chem. Phys.*, 2012, **14**, 2762–2768

www.rsc.org/pccp

**PAPER**

# Polymer dynamics in responsive microgels: influence of cononsolvency and microgel architecture

**C. Scherzinger,[a] O. Holderer,[b] D. Richter*[c] and W. Richtering*[a]**

***Received 21st October 2011, Accepted 3rd January 2012***
**DOI: 10.1039/c2cp23328b**



The dynamics of polymers on the nm and ns scales inside responsive microgels was probed by means of Neutron Spin Echo (NSE) experiments. Four different microgels were studied: poly(*N*-isopropylacrylamide) (PNIPAM) and poly(*N*,*N*-diethylacrylamide) (PDEAAM) microgels, a P(NIPAM-*co*-DEAAM) copolymer microgel and a core–shell microgel with a PDEAAM core and a PNIPAM shell. These four different microgel systems were investigated in a $D_2O/CD_3OD$ solvent mixture with a molar $CD_3OD$ fraction of $x_{MeOD} = 0.2$ at 10 °C. The PNIPAM and the P(NIPAM-*co*-DEAAM) microgels are in the collapsed state under these conditions. They behave as solid diffusing objects with only very small additional contributions from internal motions. The PDEAAM particle is swollen under these conditions and mainly Zimm segmental dynamics can be detected in the intermediate scattering function at high momentum transfer. A cross-over to a collective diffusive motion is found for smaller *q*-values. The shell of the PDEAAM-core–PNIPAM-shell particle is collapsed, which leads to a static contribution to $S(q,t)$; the core, however, is swollen and Zimm segmental dynamics are observed. However, the contributions of the Zimm segmental dynamics to the scattering function are smaller as compared to the pure PDEAAM particle. Interestingly the values of the apparent solvent viscosities inside the microgels as obtained from the NSE experiments are higher than for the bulk solvent. In addition different values were obtained for the PDEAAM microgel, and the PDEAAM-core of the PDEAAM-core–PNIPAM-shell particle, respectively. We attribute the strongly increased viscosity in the PDEAAM particle to enhanced inhomogeneities, which are induced by the swelling of the particle. The different viscosity inside the PDEAAM-core of the PDEAAM-core–PNIPAM-shell microgel could be due to a confinement effect: the collapsed PNIPAM-shell restricts the swelling of the PDEAAM-core and may modify the hydrodynamic interactions in this restricted environment inside the microgel.

## Introduction

*Microgels* are sub-micron sized, cross linked polymer particles with a fuzzy structure and surface, they were studied widely in the recent years by, light scattering, neutron scattering, infrared spectroscopy, and other methods.[1–3] With these methods size, shape, morphology or composition of the particles can be identified. Some of those microgel particles show temperature dependent phase behaviour or thermo sensitivity: at the volume phase transition temperature (VPTT), the polymer becomes insoluble in a certain solvent; this process is associated with a reduction of the particle radius. The most studied thermosensitive microgel is poly(*N*-isopropylacrylamide) (PNIPAM), it has a VPTT at 32 °C in water. PNIPAM is often used as a model for denaturation of proteins; also applications as drug carrier are discussed.[4] Poly(*N*,*N*-diethylacrylamide) (PDEAAM), which has a slightly different structure, has better biocompatibility and a lower VPTT at 26 °C.[5] Copolymers of *N*-isopropylacrylamide (NIPAM) and *N*,*N*-diethylacrylamide (DEAAM) show a reduced VPTT in water compared to the homopolymers; this is related to cooperative H-bonds in the polymer chain.[5,6] In a core–shell particle both polymers are spatially separated, however the compartments of the particle can influence each other. If a collapse of the shell is induced and the core is still in the swollen state, the shell applies a certain force on the core, similarly a core can influence the shell during its phase transition.[7–11] In the collapsed state the solvent content in the microgel is strongly reduced compared to the swollen state. Nevertheless there is still a certain amount of solvent in the particle.

[a] *Institute of Physical Chemistry, RWTH Aachen University, Landoltweg 2, 52056 Aachen, Germany. E-mail: richtering@rwth-aachen.de*
[b] *Jülich Centre for Neutron Science JCNS, Forschungszentrum Jülich GmbH, Outstation at FRM II, Lichtenbergstr. 1, 85747 Garching, Germany*
[c] *Jülich Centre for Neutron Science JCNS (JCNS-1) & Institute for Complex Systems (ICS), Forschungszentrum Jülich GmbH, D-52425 Jülich, Germany. E-mail: D.Richter@fz-juelich.de*

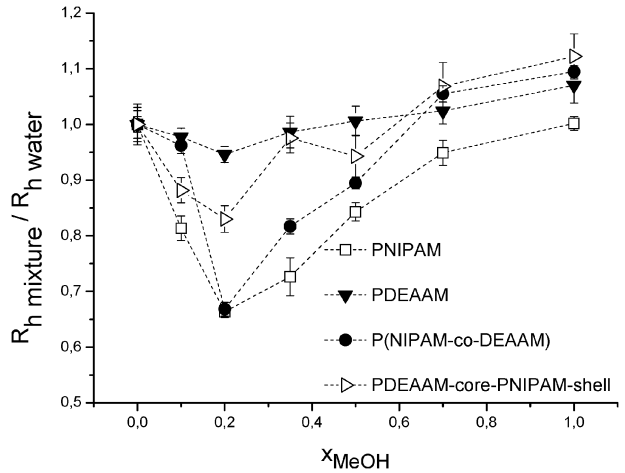


**Fig. 1** Cononsolvency effect on the hydrodynamic radius of the microgels in different $H_2O/CH_3OH$ mixtures at 10 °C, measured with DLS; PNIPAM (open squares), PDEAAM (triangle), P(NIPAM-*co*-DEAAM) (circle) and PDEAAM-core–PNIPAM-shell (open triangle).

*Cononsolvency*. The swelling behaviour of these thermo sensitive microgels can also be influenced by the composition of the solvent. Methanol ($CH_3OH$) and water ($H_2O$) are good solvents at room temperature on their own but in certain mixtures of them a PNIPAM particle becomes insoluble and collapses at room temperature. This behaviour, called cononsolvency, attracted increasing attention recently.[12–14] Most studies are concerned with linear polymers often in $H_2O$/alcohol mixtures.[15–17] In contrast to linear polymers, microgels do not always precipitate[18] and the polymer–solvent interactions are thus easier to study.

In Fig. 1 the cononsolvency behaviour of the microgels used in this publication is shown.[19] The relative hydrodynamic radius (hydrodynamic radius in mixture divided by hydrodynamic radius in water) of PNIPAM, PDEAAM, P(NIPAM-*co*-DEAAM) and PDEAAM-core–PNIPAM-shell, measured with DLS, is plotted *vs.* the molar $CH_3OH$ fraction $x_{MeOH}$. PNIPAM and P(NIPAM-*co*-DEAAM) show a strong response to the addition of $CH_3OH$ while PDEAAM is almost unaffected. The PDEAAM-core–PNIPAM-shell polymer shows a reduction in size but no full collapse. The PNIPAM shell is affected by the solvent composition and collapses in certain mixtures, the PDEAAM core stays in the swollen state. This was also supported by SANS data and the corresponding fit of the PDEAAM-core–PNIPAM-shell particle.[19] The absolute hydrodynamic radii of the microgels measured with DLS at 10 °C are listed in Table 1. At 10 °C the relative radius of the particles is the smallest at a methanol fraction of $x_{MeOH} = 0.2$, as shown in Fig. 1. Therefore this concentration was chosen to investigate the samples with NSE. The cononsolvency effect is used to collapse the solvent sensitive polymer part of the microgels without changing the temperature.

**Table 1** Absolute hydrodynamic radii in nm of the microgel particles in different solvents at 10 °C

| | PNIPAM | PDEAAM | P(NIPAM-*co*-DEAAM) | PDEAAM-core–PNIPAM-shell |
|---|---|---|---|---|
| $H_2O$ | 71 ± 2.2 | 87 ± 2 | 81 ± 3 | 229 ± 3.2 |
| $x_{MeOH} = 0.1$ | 58 ± 1.6 | 85 ± 1.3 | 78 ± 1.2 | 202 ± 5.1 |
| $x_{MeOH} = 0.2$ | 47 ± 0.8 | 82 ± 1.2 | 54 ± 1 | 190 ± 5.5 |
| $x_{MeOH} = 0.35$ | 52 ± 2.5 | 86 ± 2.5 | 66 ± 1.1 | 224 ± 6.2 |
| $x_{MeOH} = 0.5$ | 60 ± 1.2 | 88 ± 2.3 | 73 ± 0.8 | 216 ± 8.6 |
| $x_{MeOH} = 0.7$ | 68 ± 1.6 | 89 ± 2 | 86 ± 1.1 | 245 ± 10 |
| $CH_3OH$ | 72 ± 0.9 | 93 ± 2.8 | 89 ± 0.9 | 257 ± 9.3 |

Depending on the length scale, which is to be observed, different scattering experiments can be accomplished. The measure of length scale in scattering experiments is the momentum transfer, or scattering vector $q$. With DLS, large scales, *i.e.* small $q$-vectors (with real space distance $d = 2\pi/q$) are accessible, and the translational diffusion coefficient ($D_{MG}$) of the entire microgel particle can be probed in this way. With static neutron scattering the structure of a particle can be revealed. With NSE dynamics of the chains constituting the particle can be studied; here we study the influence of the swelling state of the microgel particle on those inner dynamics, by comparing collapsed PNIPAM and swollen PDEAAM in a deuterium oxide/methanol-d4 mixture with 20% methanol-d4 at a constant temperature of 10 °C. Moreover the influence of particle architecture (copolymer *vs.* core–shell) on the polymer chain dynamics is very interesting and we investigate if it is possible to achieve compartment restricted behavior in core–shell particles by the cononsolvency effect.

*Neutron Spin Echo* (NSE) spectroscopy is a technique to detect directly energy changes of a neutron due to scattering, it provides the highest energy resolution in neutron scattering and gives thus access to dynamic processes on the nanometre and nanosecond length- and timescale. In our NSE experiment we probe scales in the range of several nm; local segment dynamics are probed for the highest $q$-values ($q_{max} = 0.15$ Å$^{-1}$ in this publication). For the smallest $q$ ($q_{min} = 0.05$ Å$^{-1}$) NSE is sensitive to the gel-like concentration fluctuations.[20,21] Interestingly, quasi-ergodic scattering is found in NSE with microgels,[22] which distinguishes NSE from dynamic light scattering where non-ergodicity effects have to be considered when gels are investigated.[23]

Different polymer particles have been studied with dynamic methods before, for example polystyrene-core–PNIPAM-shell particles with depolarized dynamic light scattering (DDSL),[24] or biological polyelectrolyte particles with NSE.[25] Already in 1998 Kratz and co-workers used NSE to study network dynamics in sensitive P(NIPAM-*co*-acrylic acid) microgels.[26] They found that the particles become micro-phase separated by temperature induced collapse. Two types of possible dynamics can be observed with NSE on a local scale in microgel systems: for high density microgels, collective fluctuations can be observed which obey a $q^2$-dependence.[27–30] PNIPAM microgels with different crosslink density were studied by Hellweg and co-workers.[22] They found that the collective diffusion ($D_c$) inside the microgel network decreases significantly with increasing cross linker concentration, for lower cross linker concentrations (1–5%) in a linear and for higher cross linker concentrations (10% and 15%) in a non-linear way.

For microgels with lower density, single chain Zimm dynamics, as described by Kanaya, with a $q^3$-dependence is observed.[30] Furthermore, static inhomogeneities have been observed in macrogels.[20] Upon heating, the macrogel, which is prepared at room temperature, collapses and thus moves

away from its state of preparation. The inhomogeneous distribution of crosslink points in the deformed gel results in an additional scattering contribution. In the case of our microgels this deformation occurs in the swollen state as they are prepared in the collapsed state.

At $x_{MeOD}$ = 0.2 PNIPAM microgels collapse, whereas the PDEAAM microgel stays in the swollen state, as has been proven by SANS and DLS.[19]

A collapsed microgel can be compared with a hard sphere; the scattered signal should therefore be dominated by translational diffusion. In contrast to that swollen microgels have sponge like morphology and internal dynamics should be visible. How the dynamics of a particle are influenced by its architecture as for example our PDEAAM-core–PNIPAM-shell microgel in comparison to the copolymer microgel was not studied so far.

## Experiments

*Materials*: NIPAM, methylenebisacrylamide (BIS), sodium dodecylsulfate (SDS) and potassium peroxodisulfate (KPS) were purchased from Sigma Aldrich, DEAAM from Polysciences, Germany. Deuterated solvents were bought from Deutero, Germany. All materials were used as received. Only twice distilled milli-q-water was used during the synthesis and the cleaning process. The size of the microgels measured with DLS is in the range of 70 to 210 nm in radius (see Table 1).

*Microgel synthesis* was described in detail before.[2,19] In a conventional emulsion polymerisation a 25 mmol total monomer (NIPAM and/or DEAAM, BIS) feed was dissolved under constant nitrogen flow and stirring at 400 rpm in 125 mL degassed, twice distilled milli-q-water. After adding 1.6 mol% surfactant (SDS) and heating to 85 °C oil bath temperature the reaction was started with 1 mol% KPS. The mixture was stirred for 6 h under constant nitrogen flow at 85 °C, afterwards cooled to room temperature under stirring, filtered over glass wool and cleaned by three cycles of centrifugation and redispersion with water. The core–shell particle was synthesised *via* a two step process. The cleaned PDEAAM core was dispersed thoroughly in degassed, twice distilled milli-q-water (8 mg mL$^{-1}$). The dispersion was heated to 85 °C oil bath temperature under constant nitrogen flow and stirring at 350 rpm. Then 80 wt% (to PDEAAM core) NIPAM, 5 mol% BIS (to monomer) and 1.3 mol% SDS were added and the mixture was stirred for 30 minutes, afterwards the reaction was started by addition of 1 mol% KPS. The reaction then proceeded like described above.

*NSE measurements* have been performed by using the J-NSE spectrometer at the FRM II research reactor in Garching, Germany.[31] Microgel dispersions with pure solvents ($D_2O$ and $CD_3OD$) and a concentration of 0.2 wt% microgel in solvents were prepared one week previous to the experiment. The measured samples were mixed from these parent dispersions shortly previous to the experiment in order to avoid evaporation of $CD_3OD$. The particles were studied at a wavelength of 8 Å and $q$ vectors from 0.05 to 0.15 Å$^{-1}$. Though relatively high concentrations (at least 0.5 wt%) are more suitable for the measurements good results could be obtained with quite low concentrations of 0.2 wt% microgel in the solvent mixture. This concentration was chosen to avoid aggregation of the particles and to keep the samples comparable to the ones used in other experiments.[19] The low concentrations however led to longer measurement times. The samples were mounted in a thermostat controlled sample environment, to have comparable settings to previous SANS and DLS experiments on the same samples the temperature was set to 10 °C.[19] The dynamics of four types of microgels in a $D_2O/CD_3OD$ mixture with $x_{MeOD}$ = 0.2 molar $CD_3OD$ fraction has been studied at 10 °C: a pure PNIPAM particle and a P(NIPAM-*co*-DEAAM) copolymer particle, for both the collapse has been observed by SANS and DLS; then a pure PDEAAM particle which is swollen in the solvent mixture at 10 °C, and a PDEAAM-core–PNIPAM-shell particle with a collapsed shell and a swollen core.

## Results

The PNIPAM and the P(DEAAM-*co*-NIPAM) sample showed a nearly pure elastic signal in the $q$- and time-window of the NSE experiment (see Fig. 2). On the left the normalized intermediate scattering function of the PNIPAM sample is plotted *vs.* the Fourier time, the right shows the same for

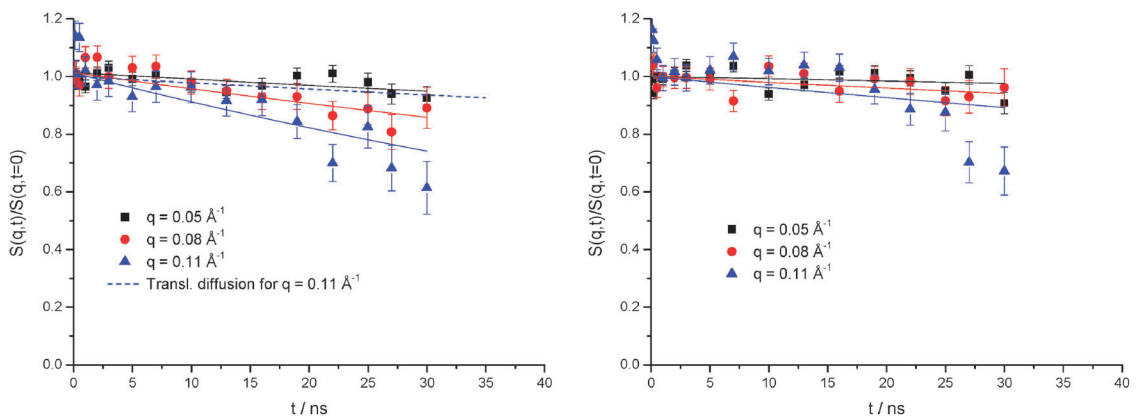


**Fig. 2** (left) $S(q,t)/S(q,t = 0)$ *vs.* the Fourier time of the PNIPAM particle in $x_{MeOH}$ = 0.2 at different $q$-vectors: the dashed line shows the contribution from translational diffusion for the highest $q$-value $q$ = 0.11; (right) $S(q,t)/S(q,t = 0)$ *vs.* the Fourier time of the P(NIPAM-*co*-DEAAM) particle in $x_{MeOH}$ = 0.2 at different $q$-vectors.

 

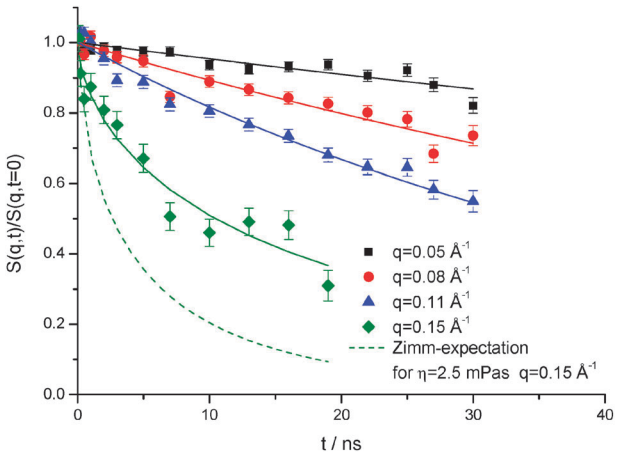


**Fig. 3** $S(q,t)/S(q,t = 0)$ *vs.* the Fourier time of a PDEAAM microgel at $q = 0.05$ (black), 0.08 (red), 0.11 (blue), 0.15 (green). Solid lines are individual fits, with $A = 0$ for $q = 0.05$, 0.08 and 0.11 (diffusive $q^2$-dependent dynamics), and $A = 1$ (Zimm segmental dynamics) for $q = 0.15$. The green dashed line indicates the expected relaxation curve for $q = 0.15$ with the solvent viscosity of 2.5 mPa s.

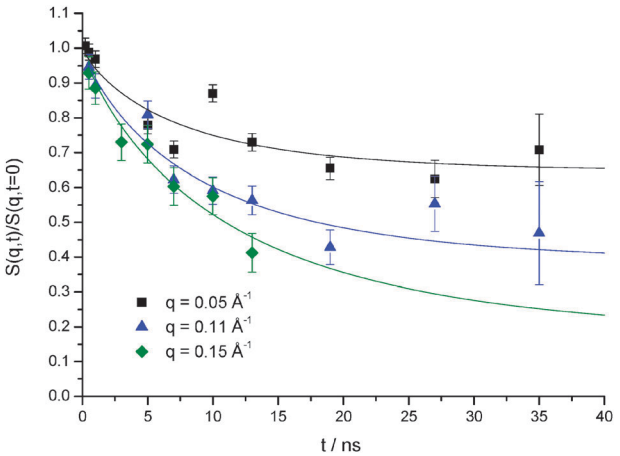


**Fig. 4** $S(q,t)/S(q,t = 0)$ *vs.* the Fourier time of the PDEAAM-core–PNIPAM-shell microgel at $q = 0.05$ (black), 0.11 (blue) and 0.15 (green). Lines are individual fits with the Zimm model plus a diffusion contribution.

P(DEAAM-*co*-NIPAM). The lowest $q$-vector measured was 0.05 Å$^{-1}$, shown in black; also 0.08 (red) and 0.11 Å$^{-1}$ (blue) were measured.

The graphs show the experimental data (dots) with a simultaneous fit (solid lines) of the three $q$-values with the intermediate scattering function

$$S(q,t)/S(q,t = 0) = \exp(-(D_{MG}q^2t))$$

with the diffusion constant $D_{MG}$, the scattering vector $q$ and the Fourier time $t$. The diffusion constants $D_{MG} = (7.45 \pm 0.8) \times 10^{-12}$ m$^2$ s$^{-1}$ for PNIPAM and $D_{MG} = (3.12 \pm 0.7) \times 10^{-12}$ m$^2$ s$^{-1}$ for the copolymer particle are larger than that deduced from DLS (Stokes–Einstein diffusion coefficient $D_{MG} = 1.8 \times 10^{-12}$ m$^2$ s$^{-1}$ for PNIPAM and $1.55 \times 10^{-12}$ m$^2$ s$^{-1}$ for the copolymer particle with the hydrodynamic radius $R_h$ at a molar MeOH concentration of 20%).

In NSE the diffusion coefficient obtained for the PNIPAM and the P(NIPAM-*co*-DEAAM) samples are faster as compared to DLS. This indicates that there is a small contribution from internal dynamics in addition to the translational particle diffusion. The NSE curves of these two samples can be rationalized in terms of rather solid particles that are in the collapsed state and have a rather compact and dense structure. Nonetheless they still contain a significant amount of solvent. This remaining solvent leads to the presence of some internal dynamics that would be missing in a completely rigid particle.

Fig. 3 displays results from the PDEAAM microgel. The intermediate scattering function of the PDEAAM microgel particle shows a significant decay in the time window of this experiment in contrast to PNIPAM and the P(NIPAM-*co*-DEAAM) samples. In addition the signal to noise ratio was better allowing investigation of an additional $q$-vector ($q = 0.15$ Å$^{-1}$). The dots represent the experimental data points and the solid lines the fits. The fits for this sample had to be done individually and will be discussed below.

Fig. 4 displays NSE results from the PDEAAM-core–PNIPAM-shell particle. As mentioned above, the scattering results from this PDEAAM-core–PNIPAM-shell particle will have contributions from the collapsed PNIPAM-shell and from the swollen core. In analogy to the collapsed, pure PNIPAM microgel particle almost no internal segmental motion should be visible for the collapsed shell of the microgel. The collapsed PNIPAM-shell with a thickness of estimated 10–20 nm will contribute elastically to the signal. The contribution from the core should be comparable to the pure PDEAAM particle. (It should be noted here that the core of the core–shell particle and the pure PDEAAM are not the same particle; nevertheless, as the synthesis conditions were the same and thus the particle densities are similar, both can be compared by using $S(q,t)/S(q,t = 0)$).

For the PDEAAM-core–PNIPAM-shell particle measurements at $q = 0.05$ Å$^{-1}$ (black), $q = 0.11$ Å$^{-1}$ (blue) and $q =$ 015 Å$^{-1}$ (green) were done. Again the dots represent the data points and the solid lines the individual fits.

The signal from the PDAAAM-core–PNIPAM-shell particle appears to decay significantly faster than the signal from the pure PDEAAM particle, at that point a rather surprising result. In order to describe the polymer dynamics in these two samples, the Zimm model for the segmental dynamics of polymers in solution is taken as the simplest minimal approach. The Zimm model describes the dynamics of a Gaussian chain in terms of a bead spring model adding the hydrodynamic interaction between the chain segments in terms of a simple Oseen tensor approach. On the proper time and length scales for the scattering function of flexible polymers in solution it provides a near quantitative description. The only free parameter in this model is the solvent viscosity.

For the analysis of the samples, that are not collapsed, the normalized intermediate scattering functions were described in terms of the following fitting function:

$$S(q,t) = \exp(-D_{MG}q^2t)(A(q)\cdot\exp(-(D_{Zimm}q^3t)^{\beta}) + (1 - A(q))\cdot\exp(-D_cq^2t)) \quad (1)$$

Different types of dynamics will contribute to eqn (1). On local length scales as measured at higher $q$-values with NSE,

polymer chains undergo Zimm motion in a solution where hydrodynamic interaction is important. The Zimm model predicts a $q^3$-dependent relaxation rate ($D_{\mathrm{Zimm}}$) and a stretched exponential relaxation. At higher crosslink-densities, when the observed length scale probes the mesh of the network, collective diffusion ($D_c$) with a $q^2$-dependent rate and a simple exponential decay is expected, as *e.g.* observed by Hellweg,[22] Adelsberger *et al.*[27] or Farago *et al.*[32] The translational diffusion of the entire microgel particle is overlying these contributions and is accounted for with the multiplicative first exponential function. The diffusion constant for the particle diffusion, $D_{\mathrm{MG}}$, has been measured with DLS and is then fixed in the further analysis. Fig. 2 shows that the contribution from $D_{\mathrm{MG}}$, even at the highest $q$-value measured for the PNIPAM particle, is only a minor contribution to the dynamics for the relatively large microgel particles in the NSE experiment.

The stretching exponent of $\beta = 0.85$ comes from a fit to the integral version of the Zimm segmental dynamics.[33] From the stretched exponential contribution one can obtain the viscosity from $D_{\mathrm{Zimm}}$ (which is obtained by the Zimm model) through relation (2)[33]

$$D_{\mathrm{Zimm}} = \frac{k_B T}{(6\pi\eta)} \frac{1}{1.354} \qquad (2)$$

The weighting factor $A(q)$ in eqn (1) tells which type of relaxation dominates, either the $q^3$-dependent Zimm-dynamics with a stretching exponent of $\beta = 0.85$,[33] or a collective diffusive $q^2$-dependent relaxation. An elastic contribution from static inhomogeneities as observed by Koizumi[20] would be represented by a finite $A(q)$ with small diffusion coefficient $D_c$. For the present experiments, it was not practicable to make an additional distinction between $q^2$- and $q^3$-dependent components and an elastic contribution. The fitting function in eqn (1) is therefore sufficient for the present purpose. The fit results are discussed below.

## Discussion

The NSE data show that the PDEAAM sample decays much faster as compared to the PNIPAM and the copolymer sample, showing clearly that the PDEAAM sample is in the swollen state with internal motion contributing to the signal. The data are analyzed in terms of the model described by eqn (1). To see if dynamic cross over effects can be observed here, the data were first fitted individually with $A = 0$ (*i.e.* $q^2$-dependent dynamics only). On large length scales, $q^2$-dependent dynamics due to the collective diffusion modes is expected to dominate, with a dynamic cross over to a $q^3$-dependent Zimm-like dynamics, when the probed length scale is approximately smaller than the average distance between crosslinks in the microgel and only the segmental dynamics is observed.

Fig. 5 shows the thus obtained relaxation rates divided by $q^2$. The $q^2$-dependence can be observed for low $q$, while for $q > 0.11$ Å$^{-1}$ a significant increase of the relaxation rate is observed. For this $q$-value the exponent $\beta$, when let free during the fitting, is found to be $\beta = 0.62 \pm 0.05$, *i.e.* a clear stretching of the curve is observed for $q = 0.15$ Å$^{-1}$. The length scale of

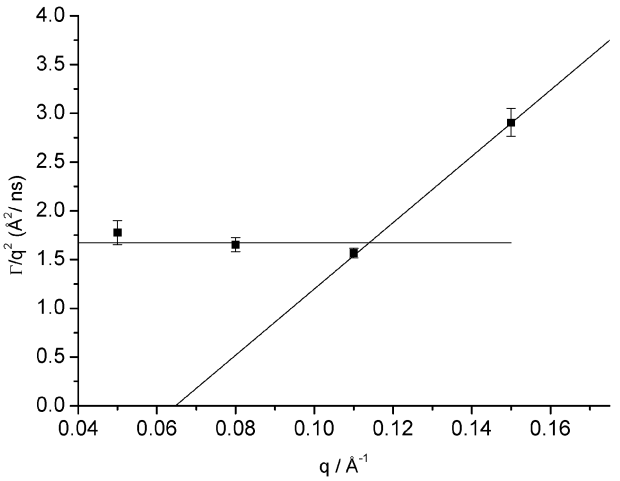


**Fig. 5** Diffusion coefficient for the PDEAAM microgel as a function of $q$. At $q \approx 0.11$ Å$^{-1}$ the cross over from diffusive motion (indicated as a plateau line in the plot) to internal Zimm-like segmental dynamics (the $q^3$-dependence appears as a linear increase in this representation).

this cross over $d = 2\pi/q = 5.7$ nm is related to the mesh size of the microgel. This shows that the PDEAAM particle is in a swollen state with segmental Zimm-like dynamics at short length scales.

The contribution of overall translational diffusion has been fixed by the diffusion coefficient from DLS measurements. The apparent viscosity of the solvent determined by the Zimm fit for $q = 0.15$ Å$^{-1}$, however, is found to be $9 \pm 2$ mPa s, *i.e.* much higher than the value of 2.5 mPa s for the $D_2O/CH_3OH$ solvent mixture, possibly indicating that the full Zimm regime is not yet reached. However, any elastic contribution would also lead to an apparent increased viscosity. The cross-over from $q^2$- to $q^3$-regime depends also on the chain density of the microgel.[22] The microgel has a distribution in the crosslink-density with a higher cross-linked core region and a less cross-linked corona.[19] This distribution of crosslink density smears out the transition from $q^2$ to $q^3$ behavior. It has been tested, if an additional elastic contribution due to static inhomogeneities can be identified in the dynamic structure factor of the PDEAAM microgel particles. With the limited time range a clear separation of dynamic and static parts was not possible. Nevertheless following the results of Koizumi such an elastic part that would lead to an increase of the microscopically observed viscosity is not unlikely.

The PDEAAM-core–PNIPAM-shell particle revealed an almost constant plateau in the time window of our experiment. Thus a slow process or elastic part is present, which is much more pronounced as compared to the PDEAAM system. This contribution attributed to scattering from the collapsed shell, which has no significant dynamic signature in the time window of this experiment. This again shows the compact nature of the PNIPAM shell in the solvent mixture.

The data of the PDEAAM-core–PNIPAM-shell have been fitted with eqn (1) with amplitude $A(q)$ as a free parameter besides $D_c$. An elastic contribution has been represented by fixing $\exp(-(D_{\mathrm{Zimm}}q^3t)^\beta)$ to 1. $A(q)$ measures the elastic contribution and $(1 - A(q))$ is the fraction of a diffusive $q^2$-contribution. We found that $A(q)$ was $0.70 \pm 0.03$ for

 

**Table 2** Relaxation rates $\Gamma$ (and fit error $\Delta\Gamma$) obtained from fits with eqn (1) for the PDEAAM microgel and the core–shell microgel. $q$ in $Å^{-1}$; $\Gamma$ in $ns^{-1}$

| $q$ | $\Gamma = Dq^2$ PDEAAM | $\Delta\Gamma$ | $\Gamma = Dq^2$ Core–shell | $\Delta\Gamma$ |
|---|---|---|---|---|
| 0.0500 | 0.0044 | 0.0003 | 0.1822 | 0.0444 |
| 0.0800 | 0.0106 | 0.0004 | — | — |
| 0.1100 | 0.0189 | 0.0006 | 0.1324 | 0.0315 |
| 0.1500 | 0.0654 | 0.0032 | 0.1438 | 0.0582 |

$q = 0.05$, $0.46 \pm 0.06$ for $q = 0.11$ and $0.38 \pm 0.13$ for $q = 0.15$ $Å^{-1}$ respectively. The elastic signal decreases with increasing $q$, obviously the swollen core dominates the signal with increasing $q$. The fitted relaxation rates are shown in Table 2.

When comparing the relaxation rates $\Gamma = Dq^2$ of the PDEAAM-sample with the core–shell particle, one notices that the core–shell particle has a significantly faster internal dynamics. The reason for this behaviour might be related to confinement effects from the collapsed PNIPAM shell, which acts like a "corset" for the swollen core.[34] The collapsed PNIPAM-shell restricts the swelling of the core as compared to the pure PDEAAM system. This restriction reduces the correlation length in the network of the PDEAAM-core as compared to the pure PDEAAM particle.[33] A similar increase of the relaxation rate of polymers under confinement has recently been observed for PEO polymers on clay platelets.[35] However, further investigations are needed to clarify this point.

The crossover from diffusive to Zimm regime of the PDEAAM core is expected to be at a slightly bigger $q$ as in the pure PDEAAM particle due to the higher density of chains induced by the compressing shell. The data for the core–shell particle are not sufficient to distinguish clearly between the two regimes. When fitting the stretching exponent in addition to an elastic contribution, it changes from a simple exponential with $\beta = 1$ for $q = 0.05$ $Å^{-1}$ and $q = 0.08$ $Å^{-1}$ to $\beta \approx 2/3$. This change in line shape is a hint that the transition between the $q^2$- to the $q^3$-regime seems to take place gradually in the $q$-window of the experiment for the PDEAAM-core–PNIPAM-shell particle.

The striking observation with the pure PDEAAM is the high apparent viscosity in the PDEAAM microgel; part of the apparent high viscosity could be a signature of static inhomogeneities in analogy to the observations in PNIPAM macrogels.[20,36,37] (With the solvent viscosity of 2.5 mPa s and an additional elastic contribution no satisfying fits could be obtained.) As mentioned above, our microgels are synthesized in the collapsed state, thus the swelling leads to an increase in network inhomogeneities. This leads to different relaxation rates of the chains in a swollen and in a collapsed microgel. The static inhomogeneities of the local gel network could thus at least partly explain the apparent high viscosity found in the PDEAAM sample with the Zimm model. The local viscosity in the PDEAAM-core of the PDEAAM-core–PNIPAM-shell microgel seems to be significantly smaller than in the case of the pure PDEAAM sample and with $\sim$5.5 mPa s (determined at the highest $q = 0.15$ $Å^{-1}$ with the Zimm model plus an elastic contribution) in between the pure solvent viscosity (2.5 mPa s) and that of the PDEAAM microgel. This might be also an effect of the confinement of the collapsed shell and the exerted "corset" force on the swollen core.

## Conclusions

Four different microgels, PNIPAM, P(NIPAM-*co*-DEAAM), PDEAAM and a PDEAAM-core–PNIPAM-shell, were studied with Neutron Spin Echo in a $D_2O/CD_3OD$ mixture with a molar $CD_3OD$ fraction of $x_{MeOD} = 0.2$ at 10 °C. Under these conditions the PNIPAM and the P(NIPAM-*co*-DEAAM) microgels are in the collapsed state and in the NSE experiments they appeared as solid diffusing objects with only very small additional contributions from internal motions.

The PDEAAM particle is swollen under these conditions and mainly Zimm segmental dynamics can be detected in its intermediate scattering function at $q > 0.11$ $Å^{-1}$ as well as a cross over to a collective diffusive motion for smaller $q$-values.

The shell of the PDEAAM-core–PNIPAM-shell particle is collapsed, this can be deduced from the static contribution in $S(q,t)$: the core, however, is swollen and this leads to a reduced fraction of Zimm segmental dynamics in the particles scattering function as compared to the pure PDEAAM particle.

Interestingly, different apparent solvent viscosities are obtained for the PDEAAM microgel, the PDEAAM-core of the PDEAAM-core–PNIPAM-shell particle and the bulk solvent. We attribute the strongly increased viscosity in the PDEAAM particle (as compared to the bulk solvent) to the increased amount of inhomogeneities induced by the swelling of the particle. The different viscosity in the PDEAAM-core of the PDEAAM-core–PNIPAM-shell particle could be a result of the confinement of the swollen PDEAAM-core by the collapsed PNIPAM-shell. Hydrodynamic interactions of the Zimm model may be modified in this restricted environment inside the particle.

## Acknowledgements

This research project has been supported by the European Commission under the 7th Framework Programme through the Key Action: Strengthening the European Research Area, Research Infrastructures. Contract no.: 226507 (NMI3). This work is based on experiments performed at the Jülich Centre for Neutron Science JCNS, Forschungszentrum Jülich, Germany.

## References

1 W. H. Blackburn and L. A. Lyon, *Colloid Polym. Sci.*, 2008, **286**, 563–569.
2 M. Stieger, W. Richtering, J. S. Pedersen and P. Lindner, *J. Chem. Phys.*, 2004, **120**, 6197–6206.
3 M. Pühse, M. Keerl, C. Scherzinger, W. Richtering and R. Winter, *Polymer*, 2010, **51**, 3653–3659.
4 R. Pelton, *Adv. Colloid Interface Sci.*, 2000, **85**, 1–33.
5 M. Keerl and W. Richtering, *Colloid Polym. Sci.*, 2007, **285**, 471–474.
6 M. Keerl, V. Smirnovas, R. Winter and W. Richtering, *Macromolecules*, 2008, **41**, 6830–6836.
7 X. Hu, Z. Tong and L. A. Lyon, *J. Am. Chem. Soc.*, 2010, **132**, 11470–11472.
8 I. Berndt, J. S. Pedersen, P. Lindner and W. Richtering, *Langmuir*, 2006, **22**, 459–468.
9 C. D. Jones and L. A. Lyon, *Langmuir*, 2003, **19**, 4544–4547.

10 I. Berndt, C. Popescu, F. J. Wortmann and W. Richtering, *Angew. Chem., Int. Ed.*, 2006, **45**, 1081–1085 (*Angew. Chem.*, 2006, **118**, 1099–1102).
11 J. Gerhardt, G. Frenning, W. Richtering and P. Hanson, *Soft Matter*, 2011, **7**, 10327–10338.
12 Y. Maeda, T. Nakamura and I. Ikeda, *Macromolecules*, 2002, **35**, 10172–10177.
13 F. Tanaka, T. Koga and F. M. Winnik, *Phys. Rev. Lett.*, 2008, **101**, 0283021–0283024.
14 J. Hao, H. Cheng, P. Butler, L. Zhang and C. C. Han, *J. Chem. Phys.*, 2010, **132**, 1549021–1549029.
15 C.-T. Tao and T.-H. Young, *Polymer*, 2005, **46**, 10077–10084.
16 F. Tanaka, T. Koga, H. Kojima, N. Xue and F. Winnik, *Macromolecules*, 2011, **44**, 2978–2989.
17 H. Kojima and F. Tanaka, *Macromolecules*, 2010, **43**, 5103–5113.
18 H. M. Crowther and B. Vincent, *Colloid Polym. Sci.*, 1998, **276**, 46–51.
19 C. Scherzinger, P. Lindner, M. Keerl and W. Richtering, *Macromolecules*, 2010, **43**, 6829–6833.
20 S. Koizumi, M. Monkenbusch, D. Richter, D. Schwahn and B. Farago, *J. Chem. Phys.*, 2004, **121**, 12721–12731.
21 O. Holderer, M. Monkenbusch, G. Borchert, C. Breuning and K. Zeitelhack, *Nucl. Instrum. Methods Phys. Res., Sect. A*, 2008, **586**, 90–94.
22 T. Hellweg, W. Eimer, S. Pouget and K. Kratz, *Lecture Notes in Physics*, in *Neutron spin echo spectroscopy. Basics, trends and applications*, ed. F. Mezei, C. Pappas and T. Gutberlet, 2003, vol. 601, pp. 291–301.
23 P. N. Pusey and B. van Megen, *Physica A (Amsterdam)*, 1989, **157**, 705–741.
24 S. Bolisetty, M. Hoffmann, S. Lekkala, T. Hellweg, M. Ballauf and L. Harnau, *Macromolecules*, 2009, **42**, 1264–1269.
25 F. Horkay, P. J. Basser, A.-M. Hecht and E. Geissler, *J. Chem. Phys.*, 2008, **128**, 1351031–1351037.
26 K. Kratz, T. Hellweg and W. Eimer, *Ber. Bunsen-Ges. Phys. Chem.*, 1998, **102**, 1603–1608.
27 J. Adelsberger, A. Meier-Koll, A. M. Bivigou-Koumba, P. Busch, O. Holderer, T. Hellweg, A. Laschewsky, P. Müller-Buschbaum and C. M. Papadakis, *Colloid Polym. Sci.*, 2011, **289**, 711–720.
28 T. Hellweg, K. Kratz, S. Pouget and W. Eimer, *Colloids Surf., A*, 2002, **202**, 223–232.
29 J. Adelsberger, A. Kulkarni, A. Jain, W. Wang, A. M. Bivigou-Koumba, P. Busch, V. Pipich, O. Holderer, T. Hellweg, A. Laschewsky, P. Müller-Buschbaum and C. M. Papadakis, *Macromolecules*, 2010, **43**, 2490–2501.
30 T. Kanaya, M. Monkenbusch, H. Watanabe, M. Nagao and D. Richter, *J. Chem. Phys.*, 2005, **122**, 1449051–1449059.
31 M. Monkenbusch, R. Schätzler and D. Richter, *Nucl. Instrum. Methods Phys. Res., Sect. A*, 1997, **399**, 301–323.
32 B. Farago, M. Molkenbusch, D. Richter, J. S. Huang, L. J. Fetters and A. P. Gast, *Phys. Rev. Lett.*, 1993, **71**, 1015–1018.
33 D. Richter, M. Monkenbusch and A. Arbe, *Adv. Polym. Sci.*, 2005, **174**, 1–221.
34 I. Berndt, J. S. Pedersen and W. Richtering, *Angew. Chem., Int. Ed.*, 2006, **45**, 1737–1741 (*Angew. Chem.*, 2006, **118**, 1769–1773).
35 X. Frielinghaus, M. Brodeck, O. Holderer and H. Frielinghaus, *Langmuir*, 2010, **26**, 17444–17448.
36 H. Tanaka, *J. Phys.: Condens. Matter*, 2000, **12**, R207–R264.
37 M. Doi and A. Onuki, *J. Phys. II*, 1992, **2**, 1631–1656.




 